Techno-Science Research Journal 12 (1) (2024) P 46-52

Content list available at ITC

Techno-Science Research Journal

Journal Homepage: http://techno-srj.itc.edu.kh/

Techno-Science Research Journal

Design of Multi-Layer Planar Electromagnetic Wave Absorber Using 1D-FDTD Integrated with ASA and Gradient Descent Optimization Method

Dara CHUN[1], Kosorl THOURN[2], Sokchenda SRENG[2]

[1] *Research Unit of Mechatronic and Information Technology, Institute of Technology of Cambodia, Russian Federation Blvd., P.O. Box 86, Phnom Penh, Cambodia*

[2] *Department of Telecommunication and Network Engineering, Institute of Technology of Cambodia, Russian Federation Blvd., P.O. Box 86, Phnom Penh, Cambodia*

Received: 16 August 2023; Accepted: 23 October 2023; Available online: June 2024

Abstract: *In this paper, an adjoint sensitivity analysis with an iterative first-order gradient descent optimization technique is proposed in conjunction with the finite-difference time-domain (FDTD) method to design a broadband multi-layer planar electromagnetic wave absorber made of expanded polystyrene mixed with graphite powder. This analysis needs an additional adjoint field simulation for the sensitivity calculation of design parameters (thickness and density of absorbing materials), which can be computed by the FDTD technique with the backward time scheme. The result obtained from the proposed design method is compared with the point frequency matching method. A smaller thickness, carbon content, and better absorption performance of a multi-layer planar absorber are obtained over the frequency range of* $0.4 - 5$ *GHz.*

Keywords: Finite-Difference Time-Domain (FDTD), Adjoint Sensitivity Analysis (ASA), Steepest Descent, Point Frequency Matching method (PFM), Multi-layer Planar Absorber

1. INTRODUCTION

Electromagnetic (EM) wave absorbers have been extensively utilized on all of the internal wall surfaces of a shielded room to create a simulated free-space environment, called an anechoic chamber. This chamber has been employed for a wide variety of EM measurements, including electromagnetic compatibility testing and/or antenna characterization [1]. Typically, the absorber used in the chamber is required to have good absorption characteristics over a broadband frequency range with a reflectivity of less than -20dB [2]. This absorption performance depends not only on material types of lossy dielectric or/and magnetic permeability but also on their structures [2] which could be planar, wedge, and/or pyramidal shapes.

A multi-layer planar shape is one of the geometry structures that have been frequently used to fabricate EM wave absorbers. This structure is convenient to implement and more flexible than other shapes. Its performance depends on the combination of thickness and electrical properties (permittivity or/and permeability) in each layer [3–9]. A number of studies have been done on the design of such an EM wave absorber. In [3], a genetic algorithm (GA) was first introduced and utilized to optimize the thickness and type of fictitious materials available from a database, in which two groups of binary bits were employed to describe thickness and material in each layer. The in-house GA was further developed [4] to design the broadband multi-layer planar EM wave absorber using carbon nanostructure-based composites (micrographite single-walled carbon nanotube, micrographite walled carbon nanotube, carbon nanofiber, and fullerene-based composite materials) with various weight percentages of conductive filler. Similar algorithms for EM absorber design and optimization can be found in [5,6]. The objective functions in [3–6] were coded to minimize not only the reflection coefficients computed by the transmission line theory but also the total thickness of the EM absorber.

The electrical properties (complex permittivity) of expanded polystyrene mixed with graphite powder [7] were measured and empirically modeled in terms of frequency and carbon content. Shimizu [8] had proposed a method based on the Newton-Raphson iterative technique called the point frequency matching (PFM) method to design a multi-layer planar EM wave absorber made of this composite material for

* Corresponding author: Dara CHUN
E-mail: dara_chun@gsc.itc.edu.kh; Tel: +855-96 435 9862

normal incidence waves. This method was further extended in [9] for oblique incident waves. Comparing to GA, the proposed method in [8,9] is simpler in implementation and can optimize the design parameters (thickness and carbon content) in continuous rather than discrete values. Most studies used transmission line theory to compute the reflection coefficient of the multi-layer planar EM wave absorber as the objective function to be utilized in the design process in the frequency domain [3−9]. However, a lack of time-domain techniques has been found in the literature for the design and optimization of the EM wave absorber made of this composite material.

One of the time-domain techniques is the finite-difference time-domain (FDTD) method [10]. This is due to its computational efficiency and ability to calculate a continuous broadband solution. Therefore, the FDTD method is considered in this work to model a multi-layer planar EM wave absorber made of expanded polystyrene mixed with graphite powder [7]. To find the optimal design parameters of such an EM absorber, an optimization method integrating with the FDTD method is required. GA [11] and adjoint sensitivity analysis (ASA) [12] have been used to find the optimal shape topology of devices in electromagnetic applications.

In this paper, the ASA technique with an iterative first-order gradient descent optimization method is applied in conjunction with the FDTD method to optimize the design parameters of a multi-layer planar EM wave absorber. The proposed design method is going to be described in section 2 by following numerical calculations, results, and discussion in section 3. Finally, a conclusion is given in section 4.

2. METHODOLGY

2.1 Multi-Layer Planar Structure EM Wave Absorber

The structure of the multi-layer planar electromagnetic wave absorber is considered and illustrated in Fig. 1. This planar absorber is composed of N layers ($n = 1,2,\dots,N$) and backed with the perfect electric conductor (PEC). Each layer is characterized by thickness (d_n) and dielectric material. The expanded polystyrene mixed with graphite (carbon) powder in [7] is adopted as the dielectric-absorbing material, whose electrical properties depend on both frequency f and carbon content G. To enable a time-domain broadband calculation of the reflectivity of an EM wave absorber [13] using the FDTD method, the empirical model of the relative complex permittivity ($\dot{\varepsilon}_r(\omega, G)$), which was derived from [7], was remodeled as a multi-pole Debye relaxation model with an additional static conductivity term (all Deby parameters are written in term of the angular frequency ω and carbon content G). The second order Debye model is considered in this study, which is mathematically expressed as follows:

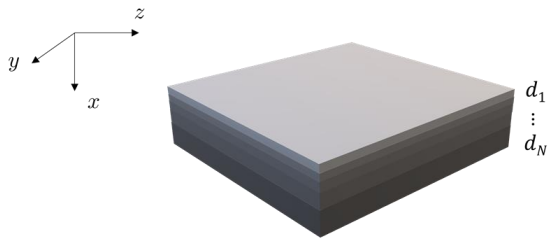

Fig. 1: Structure of the multi-layer planar electromagnetic wave absorber

$$\dot{\varepsilon}_r(\omega, G) = \varepsilon_\infty(G) + \sum_{p=1}^{2} \frac{\Delta\varepsilon_p(G)}{1 + j\omega\tau_p(G)} + \frac{\sigma_0(G)}{j\omega\varepsilon_0} \quad \text{(Eq. 1)}$$

where $\varepsilon_\infty(G)$ represents extremely high frequency permittivity, $\tau_p(G)$ represents the relaxation period, $\Delta\varepsilon_p(G)$ represents relaxation strength, and $\sigma_0(G)$ represents the electric static conductivity.

2.2 Maxwell's Equations

Assume that the dimensions of the multi-layer planar wave absorber (see in Fig. 1) in y and z directions are infinite lengths, hence, the absorber can be modeled by the 1D-FDTD method. With the x-directed wave propagation and z-polarized electric field, the EM field equations in Debye medium can be described mathematically as:

$$\mu_0 \frac{\partial H_y}{\partial t} = \frac{\partial E_z}{\partial x} \quad \text{(Eq. 2)}$$

$$\varepsilon_0\varepsilon_\infty \frac{\partial E_z}{\partial t} + \sigma_0 E_z + \sum_{p=1}^{2} J_{z,p} = \frac{\partial H_y}{\partial x} \quad \text{(Eq. 3)}$$

$$\tau_p \frac{\partial J_{z,p}}{\partial t} + J_{z,p} = \varepsilon_0 \Delta\varepsilon_p \frac{\partial E_z}{\partial t} \quad \text{(Eq. 4)}$$

where $\varepsilon_0 = 8.85 \times 10^{-12}\ F/m$ and $\mu_0 = 4\pi \times 10^{-7}\ H/m$ are represented as free space permittivity and permeability, respectively. E_z, H_y, and $J_{z,p}$ (for $p = 1,2$) are represented as the electric field, the magnetic field, and the polarization current, respectively.

2.3 The Objective Function

In order to estimate the design parameters, an objective function is required and mathematically determined as

$$F = \int_0^{T_m} \phi(\boldsymbol{d}, \boldsymbol{G}, \boldsymbol{V})\, dt \quad \text{(Eq. 5)}$$

where $\boldsymbol{d} = [d_1, d_2, \dots, d_n]$, and $\boldsymbol{G} = [G_1, G_2, \dots, G_n]$, for $n = 1,2, \dots, N$, are vectors of design parameters containing thickness and carbon content in each layer of the multilayer planar wave absorber to be optimized, respectively; and $\boldsymbol{V} = [H_y, E_z, J_{z,1}, J_{z,2}]^T$ is a vector of state variables that contains electric and magnetic fields, and polarization current. In this design, the kernel function ϕ is taken in the form of the energy difference between the computed and observed electric fields, which is expressed as

$$\phi(\boldsymbol{d}, \boldsymbol{G}, E_z) = \frac{1}{2}(E_z - E_z^{obs})^2 \qquad \text{(Eq. 6)}$$

where E_z is the computed electric field (total field), which is implicitly a function of d_n and G_n. The observed electric field (incidence field) is represented as E_z^{obs}, which is an implicitly a function of d_n. In order obtain the desire response, the objective function need to be minimized by the adjoint sensitivity analysis as explained in the following section.

2.4 Adjoint Sensitivity Analysis (ASA)

The analytical derivative (sensitivity) of the objective function in Eq. 5 with respect to the n-th parameters can be described mathematically as

$$\frac{\partial F}{\partial d_n} = \int_0^{T_m} \frac{\partial^e \phi}{\partial d_n} dt + \int_0^{T_m} \left(\frac{\partial \phi}{\partial \boldsymbol{V}}\right)^T \frac{\partial \boldsymbol{V}}{\partial d_n} dt \qquad \text{(Eq. 7)}$$

$$\frac{\partial F}{\partial G_n} = \int_0^{T_m} \frac{\partial^e \phi}{\partial G_n} dt + \int_0^{T_m} \left(\frac{\partial \phi}{\partial \boldsymbol{V}}\right)^T \frac{\partial \boldsymbol{V}}{\partial G_n} dt \qquad \text{(Eq. 8)}$$

where T_m is the time over which the system response is observed. The first integrals in both equations are the explicit dependance on the parameters. This explicit dependence is nonzero only if the kernel function ϕ contains d_n and G_n. The second integrals are the implicit terms which can be solved using the adjoint variable methods [14,15]. Then, the sensitivity of the objective function with respect to d_n and G_n can be mathematically rewritten as follows:

$$\frac{\partial F}{\partial d_n} = \int_0^{T_m} \frac{\partial^e \phi}{\partial d_n} dt - \int_0^{T_m} \boldsymbol{\lambda}^T \left(\frac{\Delta \boldsymbol{R}_n}{\Delta d_n}\right) dt \qquad \text{(Eq. 9)}$$

$$\frac{\partial F}{\partial G_n} = \int_0^{T_m} \frac{\partial^e \phi}{\partial G_n} dt - \int_0^{T_m} \boldsymbol{\lambda}^T \left(\frac{\Delta \boldsymbol{R}_n}{\Delta G_n}\right) dt \qquad \text{(Eq.10)}$$

where $\Delta \boldsymbol{R}_n = \Delta \boldsymbol{M}_n \dot{\boldsymbol{V}} + \Delta \boldsymbol{K}_n \boldsymbol{V}$ is the temporal residue vector associated with the parameters d_n and G_n, in which $\dot{\boldsymbol{V}} = [\dot{H}_y, \dot{E}_z, \dot{J}_{z,1}, \dot{J}_{z,2}]^T$ a vector of the state variable derivative with respect to time ($\dot{\boldsymbol{V}} = \partial \boldsymbol{V}/\partial t$); and $\Delta \boldsymbol{M}_n$ and $\Delta \boldsymbol{K}_n$, resulted from the perturb parameters Δd_n and ΔG_n, are the perturbation of the system coefficient matrices $\boldsymbol{M}$ and $\boldsymbol{K}$. These matrices are expressed as follows:

$$\boldsymbol{M}_n = \begin{bmatrix} \mu_0 & 0 & 0 & 0 \\ 0 & \varepsilon_0 \varepsilon_\infty(G_n) & 0 & 0 \\ 0 & -\varepsilon_0 \Delta\varepsilon_1(G_n) & \tau_1(G_n) & 0 \\ 0 & -\varepsilon_0 \Delta\varepsilon_2(G_n) & 0 & \tau_2(G_n) \end{bmatrix},$$

$$\boldsymbol{K}_n = \begin{bmatrix} 0 & -\partial/\partial x & 0 & 0 \\ -\partial/\partial x & \sigma_0(G_n) & 1 & 1 \\ 0 & 0 & 1 & 0 \\ 0 & 0 & 0 & 1 \end{bmatrix};$$

and $\boldsymbol{\lambda} = [\lambda_{H_y}, \lambda_{E_z}, \lambda_{J_{z,1}}, \lambda_{J_{z,2}}]^T$ is the adjoint fields vector containing the adjoint electric and magnetic fields, and the polarization currents, which is required an additional FDTD simulation for the adjoint field by running backward in time. The Eq. 7 and Eq. 8 cannot be evaluated unless the original field is performed.

2.5 Iterative first-order gradient descent optimization method

With the computed derivative of the objective function by the ASA, the updated design parameters d_n and G_n at each iteration k can be computed using the first-order gradient descent optimization method and are mathematically expressed as

- The updated value of thickness

$$d_n^{k+1} = d_n^k - \gamma^k(d_n^k)\nabla F(d_n^k) \qquad \text{(Eq. 11)}$$

- The updated value of carbon content

$$G_n^{k+1} = G_n^k - \gamma^k(G_n^k)\nabla F(G_n^k) \qquad \text{(Eq. 12)}$$

where $\nabla F(d_n^k) = \partial F/\partial d_n^k$ and $\nabla F(G_n^k) = \partial F/\partial G_n^k$ are the gradient of the objective function with respect to each design parameter; γ^k is the adaptive step size, which is mathematically defined as

$$\gamma^k = \frac{\gamma_0}{\sqrt{\sum_k (\eta^k)^2}},$$

in which $\eta^k = \nabla F$ is the weight of the gradient, γ_0 is an initial step size for updating the design parameters (d_n^k, G_n^k), $\gamma_0 \in]0,1[$.

3. NUMERICAL CALCULATION AND RESULTS

3.1 Numerical Calculation

Fig. 2 shows the flowchart of the design process of the multi-layer planar wave absorber, which performs by the 1D-FDTD integrated with the ASA method to determine the optimal values of n-layer thickness (d_n) and carbon content

(G_n). The input number of layers is the starting point of the whole process design. If input $n = 1$, this means that one-layer wave absorber is taken into account with two design parameters (d_1 and G_1). If input $n = 2$, this means that two-layer wave absorber is taken into account with four design parameters (d_1, d_2 and G_1, G_2). Then, if input n this means that n-layer wave absorber is taken into account with $2n$ design parameters ($d_1, d_2, \dots, d_n$ and $G_1, G_2, \dots, G_n$). Three separate FDTD simulations are needed in every iteration of searching for the optimal values of thickness d_n and carbon content G_n, to obtain the total electric field, the incident electric field, and the adjoint electric field. Given the number of layers n and the initial values for d_n and G_n of each layer, the computational problem space can be created.

By keeping the wave absorber and PEC as shown in Fig. 3 for the first simulation, the FDTD for the total field (including the incident and reflected fields) is then obtained by recording the electric field at the front layer interface of the planar wave absorber. The right side of the calculation model is terminated by the PEC boundary condition, while the left side is terminated by the convolutional perfectly matched layer (CPML) [10], which is utilized as the ABC. This CPML consists of 10 cells with third-order polynomial grading ($m = 3$) and its other parameters are chosen as $\kappa_{max} = 5.0$, $\sigma_{max} = 0.8(m+1)/\eta_0\Delta x$ ($\eta_0 = \sqrt{\mu_0/\varepsilon_0}$ is free-space characteristic impedance), and $\alpha_{max} = 0.05$. Each layer is characterized by thickness d_n and the second-order Debye parameters $(\varepsilon_p, \Delta\varepsilon_p, \tau_p, \sigma_0)$ for $p = 1,2$ and $n = 1,2,3, \dots, N$ (where N denotes the total number of layers). The Debye parameters depend only on n-layer carbon content G_n which $G_n \in [2,30]$ kg/m^3. The sine-modulated Gaussian pulse is mathematically written as

$$E_z(t) = \sin[2\pi f_c(t - t_c)]\, e^{-(t-t_c)^2/t_d^2}, \qquad \text{(Eq. 13)}$$

where the carrier frequency $f_c = 2.7$ GHz, bandwidth $\Delta f = 4.6$ GHz (corresponding to 10% of its maximum magnitude spectrum), the pulse length $t_d = 0.966/\Delta f$, and time shift $t_c = 4.5t_d$. This pulse is injected into the computational domain at a distance of $d_0/2 = 0.75$ m far away from the first layer of the multi-layer planar wave absorber, via the total-field (TF) formulation. The spatial discretization of the computational domain with a cell size of the $\Delta x = 1$ mm. The stability of the simulation is essential; to ensure stability, the time step is defined as $\Delta t = 0.95\Delta x/c_0$ ($c_0 = 1/\sqrt{\mu_0\varepsilon_0}$ is the speed of light in free space).

In the second FDTD simulation, the wave absorber and PEC in Fig. 3 are removed and replaced by the absorbing boundary condition (ABC) at the most right-end of the computational domain (see Fig. 4). Then, the electric field recorded at the same point as in the first simulation is considered as the incident field. With the obtained total and incident fields, the objective function can be evaluated. If the defined criteria of the objective function and maximum magnitude of the difference between computed and observed fields are not satisfied, the third FDTD simulation will be performed backward in the time domain to generate the FDTD adjoint electric field recorded at the same point as in the first simulation. This adjoint field simulation depends on the response of the original field at the observation point. The excitation source of the adjoint field simulation is determined

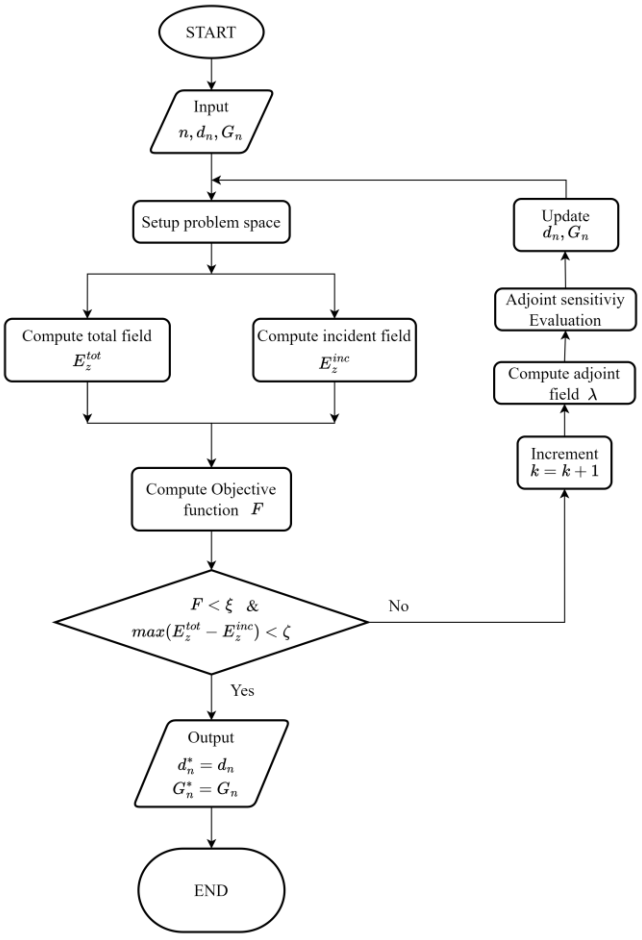

Fig. 2: Flowchart of the design process

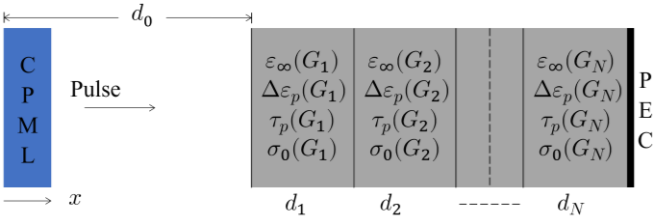

Fig. 3: Calculation model for the multi-layer planar wave absorber using the 1D-FDTD technique

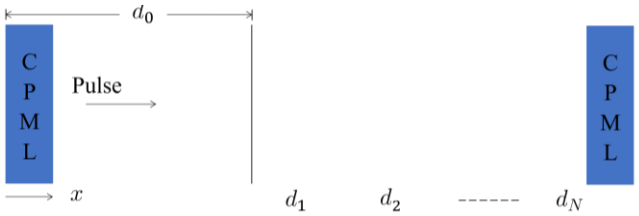

Fig. 4: Calculation model for the free space using the 1D-FDTD technique

while running the original field, with carriers carrying the information of d_n and G_n (recorded electric field of the first simulation). Due to the reverse time of the adjoint FDTD simulation, the excitation source must propagate backward in the time domain. Then, the ASA technique is evaluated using Eq. 9 and Eq. 10. With the ASA obtained, the new values of d_n and G_n can be updated by Eq. 11 and Eq. 12. This process is repeated till the optimal values of d_n and G_n are found. To compute the reflection coefficient of the planar absorber, the FDTD simulation obtained is computed via:

$$\tilde{\Gamma}(f) = \frac{\tilde{E}_{ref}(f)}{\tilde{E}_{inc}(f)}, \qquad \text{(Eq. 14)}$$

with

$$\tilde{E}_{ref}(f) = \tilde{E}_{tot}(f) - \tilde{E}_{inc}(f),$$

$$\tilde{E}_{total}(f) = DFT\{E_z^{tot}\},$$

$$\tilde{E}_{inc}(f) = DFT\{E_z^{inc}\}.$$

where $\tilde{E}_{tot}$, $\tilde{E}_{inc}$, and $\tilde{E}_{ref}$ are the spectra of the total, incident, and reflected fields, respectively; $DFT\{\cdot\}$ represents the discrete Fourier transform operator; E_z^{tot} and E_z^{inc} represent the total and incident fields captured at a record point during the FDTD simulation.

3.2 Simulation Results and Discussion

The results obtained from the proposed 1D-FDTD integrated with the ASA method are compared with those of the point frequency matching (PFM) method.

Fig. 5 shows the reflection coefficients of (a) one-layer to (e) five-layer obtained from the 1D-FDTD integrated with the ASA method and PFM computed over the frequency range 0.4−5 GHz. A very similar reflection coefficient between both methods can be observed; that is, one obtained from the proposed time-domain design method looks like the frequency shift of that obtained from the PFM method. According to the results obtained from both methods, the maximum magnitude of the reflectivity with less than -20 dB decreases wider over a wide frequency range of 0.4−5 GHz

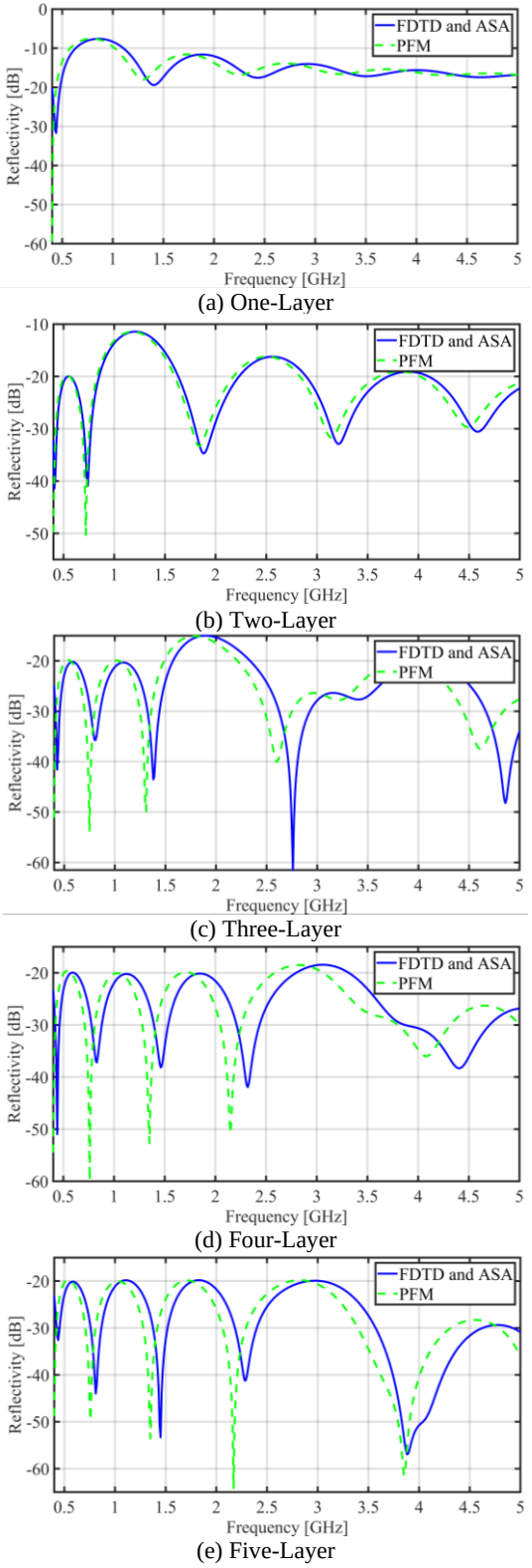

(a) One-Layer

(b) Two-Layer

(c) Three-Layer

(d) Four-Layer

(e) Five-Layer

Fig. 5: Comparison of the broadband reflection coefficient of 1-layer to 5-layer obtained by 1D-FDTD integrated with ASA and the PFM methods over 0.4−5 GHz

TABLE I: Thickness d_n(mm) and G_n(kg/m^3) in each layer of the wave absorber (from $N = 1$ to $N = 5$) for a normal incident wave obtained by 1D-FDTD integrated with ASA

	n	1	2	3	4	5
$N=1$	d_n	118.9379	–	–	–	–
	G_n	12.1906	–	–	–	–
$N=2$	d_n	104.1576	71.1482	–	–	–
	G_n	5.1045	22.8520	–	–	–
$N=3$	d_n	71.4281	57.3018	53.4109	–	–
	G_n	3.4196	9.4480	27.4577	–	–
$N=4$	d_n	46.0775	40.4799	43.6908	49.9885	–
	G_n	2.9114	5.4033	10.8606	28.3724	–
$N=5$	d_n	12.5250	40.7399	39.1344	43.8910	48.7084
	G_n	2.0295	3.2785	5.4465	10.8625	28.2163

TABLE II: Thickness d_n(mm) and G_n(kg/m^3) in each layer of wave absorber (from $N = 1$ to $N = 5$) for normal incident wave obtained by PFM

	n	1	2	3	4	5
$N=1$	d_n	126.5476	–	–	–	–
	G_n	12.4096	–	–	–	–
$N=2$	d_n	105.8386	72.2714	–	–	–
	G_n	5.2283	22.9978	–	–	–
$N=3$	d_n	73.4501	60.6653	55.7619	–	–
	G_n	3.6556	9.4782	27.6146	–	–
$N=4$	d_n	49.4807	42.9712	47.5493	53.0626	–
	G_n	3.1132	5.5068	10.8580	28.3232	–
$N=5$	d_n	14.5521	41.1875	40.1926	46.9192	53.0180
	G_n	2.0373	3.3446	5.6553	10.8990	28.3334

as the number of planar absorber layers and carbon content increase. However, to satisfy the criteria for the multi-layer planar absorber over a wide frequency range of 0.4−5 GHz with a reflectivity of -20 dB, five layers are needed to fill the whole broadband frequency.

TABLE I and TABLE II list down the optimal values d_n and G_n designed by the proposed time domain method and by obtained by the proposed time-domain method is thinner than that obtained by the PFM method. Specifically, the total thickness of the planar absorber from $N = 1$ to $N = 5$ obtained by the proposed time-domain method is 118.9379 mm, 175.3058 mm, 182.1408 mm, 180.2367 mm, and 184.9987 mm, while those obtained by the PFM method are 126.5475 mm, 178.3942 mm, 190.1355 mm, 193.4085 mm, and 196.4010 mm, respectively. Hence, the absorbers designed by the proposed time-method from $N = 1$ to $N = 5$ are thinner compared to the PFM method at around 7.6097 mm, 3.0884 mm, 7.9947 mm, 13.1718 mm, and 11.4023 mm, respectively. On the other hand, the optimal values of the total carbon content from $N = 1$ to $N = 5$ can also be obtained by the proposed time-domain method: 12.1906 kg/m^3, 27.9565 kg/m^3, 40.3253 kg/m^3, 47.5477 kg/m^3, and 49.8333 kg/m^3, while those obtained by the PFM method are 12.4095 kg/m^3, 28.2492 kg/m^3, 40.7738 kg/m^3, 47.9190 kg/m^3, and 50.5503 kg/m^3, respectively. Therefore, the absorbers designed by the proposed time-method from $N = 1$ to $N = 5$ are lower compared to the PFM method at around 0.2189 kg/m^3, 0.2927 kg/m^3, 0.4485 kg/m^3, 0.3713 kg/m^3, and 0.7170 kg/m^3. With the smaller values of d_n and G_n, the weight of the absorber can be reduced by the proposed method.

4. COCLUSIONS

In this paper, the 1D-FDTD is integrated with ASA method is proposed to design a multi-layer planar electromagnetic wave absorber. A similar reflectivity between the proposed time domain and the PFM methods can be obtained over a wide frequency range. According to the results obtained from both methods, as the number of layers and carbon content in the multi-layer planar structure increase, the reflection coefficient decreases to less than -20 dB with a wider frequency range of 0.4−5 GHz. However, five layers are needed to fill the whole broadband frequency with maximum reflectivity peaks less than -20 dB. Furthermore, the optimal thickness and carbon content obtained by the proposed time-domain method are smaller and lower than those obtained by the PFM method for planar wave absorbers, which is expected to be lighter.

In future work, with these optimal values obtained, the multi-layer planar EM wave absorber will be fabricated, and the proposed time-domain method will be extended to design wedge and pyramidal electromagnetic wave absorbers.

ACKNOWLEDGMENTS

The author would like to thank the Higher Educational Improvement Project (HEIP), IDA Credit No. 6221-KH, for providing financial support for this study.

REFERENCES

[1] Shimizu, Y. (1992). Anechoic chambers for EMI test. *IEICE Transactions on Communications*, E75-B(3), 101–106.

[2] Holloway, C. L., Delyser, R. R., German, R. F., Mckenna, P., & Kanda, M. (1997). Comparison of Electromagnetic Absorber Used in Anechoic and Semi-Anechoic Chambers for Emissions and Immunity Testing of Digital Devices. *IEEE Transactions on Electromagnetic Compatibility*, 39(1), 33.

[3] Michielssen, E., Sajer, J.-M., Ranjithan, S., & Mittra, R. (1993). Design of Lightweight, Broad-Band Microwave Absorbers Using Genetic Algorithms. *IEEE Transactions on Microwave Theory and Techniques*, 41(617), 1024–1031.

[4] Micheli, D., Pastore, R., Apollo, C., Marchetti, M., Gradoni, G., Primiani, V. M., & Moglie, F. (2011). Broadband electromagnetic absorbers using carbon nanostructure-based composites. *IEEE Transactions on Microwave Theory and Techniques*, 59(10), 2633–2646.

[5] Goudos, S. K., & Sahalos, J. N. (2006). Microwave absorber optimal design using multi-objective particle swarm optimization. *Microwave and Optical Technology Letters*, 48(8), 1553–1558.

[6] Yigit, E., & Duysak, H. (2019). Determination of Optimal Layer Sequence and Thickness for Broadband Multilayer Absorber Design Using Double-Stage Artificial Bee Colony Algorithm. *IEEE Transactions on Microwave Theory and Techniques*, 67(8), 3306–3317.

[7] Shimizu, Y., & K. Suetake. (1970). The practical wide band absorbing wall using dielectric material. *IEICE Transactions*, J53-B(3), 143–150.

[8] Shimizu, Y., & K. Suetake. (1979). A Design of multi-layer wave-absorber by point frequency matching method. *IEICE Transaction*, J62-B(4), 428–434.

[9] Aoyagi, T., & Shimizu, Y. (1995). Design of multilayer wave absorber for oblique incidence using the point frequency matching method. *Electronics and Communications in Japan Part I*, 78(3), 105–114.

[10] Taflove, A., & Hagness, S. C. (2005). Computational Electrodynamic: The Finite-Difference Time-Domain Method (Inc, Ed.; 3rd ed.). Artech House.

[11] Sui, S., Ma, H., Wang, J., Pang, Y., & Qu, S. (2015). Topology optimization design of a lightweight ultra-broadband wide-angle resistance frequency selective surface absorber. *Journal of Physics D: Applied Physics*, 48(21), 215101.

[12] Chung, Y.-S., Cheon, C., Park, I.-H., & Hahn, S.-Y. (2000). Optimal Shape Design of Microwave Device Using FDTD and Design Sensitivity Analysis. *IEEE Transactions on Microwave Theory and Techniques*, 48(12).

[13] Thourn, K., Aoyagi, T., & Takada, J. (2018). Development of Broadband Parametric Permittivity Model of Dielectric Absorbing Material for Time-domain Electromagnetic Wave Simulation. *IEEJ Transaction on Fundamental Materials*, 138(6), 302–308.

[14] Bakr, M., Elsherbeni, A., & Demir, V. (n.d.) (2017). Adjoint Sensitivity Analysis of High Frequency Structures with MATLAB. SciTech Publishing, Edison.

[15] Bakr, M. H., & Nikolova, N. K. (2004). An Adjoint Variable Method for Time-Domain Transmission-Line Modeling with Fixed Structured Grids. *IEEE Transactions on Microwave Theory and Techniques*, 52(2), 554–559.